Analytical Methods for Mathematical Modeling of Dye-Sensitized Solar Cells (DSSCs) Performance for Different Local Natural Dye Photosensitizers

J. B. Yerima[1,a], S. C Ezike[1], Dunama William[2], and Alkali Babangida[3]

[1]Department of Physics, Modibbo Adama University Yola, Nigeria

[2]Department of Mathematics, Modibbo Adama University Yola, Nigeria

[3]Department of Science Education, COE Azare, Bauchi State, Nigeria

[a]Email: bjyerima@gmail.com

Abstract. *In this paper, a new approach to generate the modified ideal diode factor of solar cells was developed which overcomes the problem of assuming its value a constant. Five models were employed to calculate the five-model parameters of one standard solar cell and fourteen DSSCs with varying photosensitizers. The results exhibit the conversion efficiencies of the solar cells studied lies in the range $2.57\% \leq \eta \leq 0.03\%$. In particular, the standard cell has the highest efficiency 3.02% followed by DSSCs with photosensitizers: bitter gourd (2.57%), mango (1%), and bougainvillea (0.83%). Also, the five model parameters calculated are all positive for El Tayyan model and the rest of the models show discrepancies of varying degrees. Furthermore, despite the existence of these discrepancies, the results reveal good fit between the model data and experimental data I-V curves. This suggests the tendency or possibility that irregular parameters may be desirable for some applications. Thus, the discrepancies found in the estimated parameters can serve as a vital assessment criterion and tool for researchers and engineers in selecting the appropriate parameter estimation method for their applications.*

Keywords: Analytical methods, Mathematical modeling, DSSCs, Photosensitizers, Irregular parameters, Conversion efficiency.

1. Introduction

The application of renewable energy is becoming more popular in modern societies and among the various sources, photoelectric energy is one of high demand in terms of increase of installed power. In addition, many specific applications such as satellites and spacecraft have motivated researchers to study the characteristics of photovoltaic cells, how to improve their power generation in the last three decades, and describe mechanisms that control the conversion of solar radiation into electric power [1-6]. Also, tremendous efforts have been made to obtain equivalent electrical/mathematical models to explain the behavior of solar cells under various conditions such as different radiation levels, photosensitizers, and cell temperatures.

An electrical model consists in a simple electric circuit whose behavior matches the real behavior of solar cell [29]. The application of circuit models together with relevant electric parameters is very crucial to optimize the power derived from the cell working under real conditions. Furthermore, the application of equivalent circuit models makes the simulation of more complicated power systems that include solar cell panels possible. In practice, in space applications these power complicated systems include batteries and programmed power consumption, with important temperature gradients and different radiation levels affecting the

output voltage of the solar cell/panel and must be maximized to ensure the survival of the spacecraft.

The photovoltaic effect leads to the conversion of sunlight radiation falling on solar cells into usable electric energy. In general, the simplest way to characterize a solar cell is by considering a current source connected in parallel to an ideal diode. The current-voltage equation that explains the theory behind the behavior of the solar cell is called Shockley's ideal diode equation given by

$$I = I_{ph} - I_o \left(e^{\frac{V}{nV_T}} - 1 \right) \qquad (1)$$

where the first term I_{ph}, is the photocurrent delivered by the constant current source, the second term is the ideal recombination current from the diffusion and recombination of electrons and holes in p-n junction sides of the cell, I_o is the reverse saturation current corresponding to it, V_T is the thermal voltage, and n is the diode ideality factor. The thermal voltage V_T is defined by

$$V_T = \frac{kT}{q} \qquad (2)$$

where T is the absolute temperature, q is the charge of the electron, and k is the Boltzmann's constant.
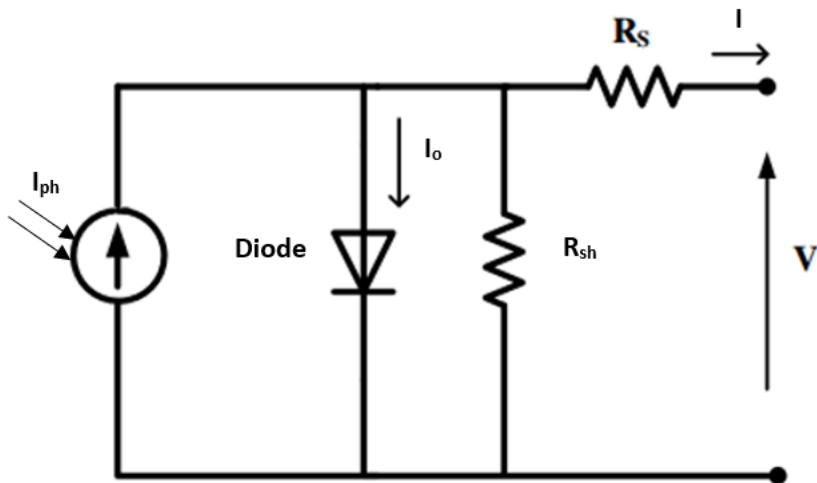

Figure 1.   Electrical equivalent circuit of the single-diode solar cell

In order to modify equation (1) to better fit the solar cell behavior, shunt resistor R_{sh} and series resistor R_s are usually added to the circuit (Fig.1). The shunt resistor is connected in parallel with the source and diode and it represents the current leakage through the high conductivity shunts across the p-n junction while the series resistor is added in series and it represents the losses in cell solder bonds, interconnection, junction box, and so on [4, 7]. Also, a dimensionless constant, n, called ideality/quality factor or emission coefficient is added to the term of the recombination current in the p- and n-sides and it takes into account the deviation of the diodes from the Shockley diffusion theory. The value of this factor depends on the ratio between current I and voltage V of the cell (10). The one-diode and two-resistors circuit model is then defined by equation (3)

$$I = I_{ph} - I_o \left[exp\left(\frac{V+IR_S}{nV_T}\right) - 1 \right] - \frac{V+IR_S}{R_{sh}} \tag{3}$$

The modified form a of the ideal factor n of the diode is defined by equation (4)

$$a = nN_sV_T = nN_s\frac{kT}{q} \tag{4}$$

where N_s is the number of solar cells connected in series i.e. N_s=1 for single-diode solar cell.

In another vein, it has been reported by some authors [8, 9] that the easiest and more commonly used 1-diode/2-resistors model exactly reveals the behavior of the solar cell around the maximum power point, that is, at high voltage levels. This model simplifies the study of the solar cell behavior as a function of the various circuit variables [10-13], and has been employed to examine the effect of the irradiance and the temperature on the cell behavior.

Once the circuit model has been selected to investigate a specific solar cell, it must be modified, that is, the value of the circuit parameters must be calculated as accurately as possible. These calculations can be based on calibration results of the cell such that once the I-V curve are obtained under definite irradiance and temperature conditions in a laboratory, the parameters of the model can be adjusted to give the best possible fit to this curve [14, 18-23, 46]. Nevertheless, sometimes the only data available to adjust the chosen circuit model comes from the manufacturer and it is restricted to only certain points on the I-V graph (short-circuit, open circuit, and maximum power points) [10, 16, 23-28]. In a nut shell, with respect to the existing methods to adjust the parameters of the chosen circuit model, some of them are numerical [11, 12, 15, 29,30, 46] while some others are analytical [2, 31-33, 45].

Analytical methods are preferred because they are simple and fast. Obviously, these methods usually rely on experimental behavior of the I-V curve, that is, they demand wide range of testing results [34]. Alternatively, some researchers have established numerical methods to adjust the electric circuit parameters to the listed characteristic point of the curve [16, 17, 22, 28]. This technique is quite motivating, as it requires only a few data to allow final users to explain the performance of photoelectric devices.

In this paper, analytical methods for photovoltaic equivalent electric circuit parameters extraction from experimental observations are reported. These approaches are based only on the points on the I-V curve (short-circuit, open circuit, and maximum power points) for modeling DSSCs performance for different local natural dye photosensitizers. The approach to the experimental parameter extraction problem for DSSC systems studied does not seem to have been studied as yet.

2. Modelings

2.1 El Tayyan Model

The El Tayyan model [35] for generating the I-V characteristics of a solar cell or PV module is given by

$$I = I_{sc} - C_1 \, e^{-\frac{V_{oc}}{C_2}} \left(e^{\frac{V}{C_2}} - 1 \right) \tag{5}$$

where C_1 and C_2 are coefficients of the model equation with units of current and voltage respectively. Using the short-circuit (SC), open-circuit (OC) and maximum power point (MPP) conditions and assuming $\frac{V_{oc}}{C_2} \gg 1 \; and \; \frac{V_{mp}}{C_2} \gg 1$ yields

$$C_1 = \frac{I_{sc} - I_{mp}}{e^{\frac{V_{mp} - V_{oc}}{C_2}}} \tag{6}$$

$$C_2 = \frac{V_{mp} - V_{oc}}{W_{-1}\left(\left(1 - \frac{V_{oc}}{V_{mp}}\right)\left(\frac{I_{mp}}{I_{sc}}\right) \right)} \tag{7}$$

where W_{-1} is the lower branch of the Lambert W function. Substituting the values of the currents and voltages at the characteristic points SC(I_{sc}, 0), OC(0, V_{oc}) and MPP(I_{mp}, V_{mp}) on the I-C curve in equations (6) and (7) the values of C_1 and C_2 can be determined. Also, substituting the values of C_1 and C_2 in equation (5) yields the desired El Tayyan empirical model for a single-diode solar model. Subsequently, for any given value of voltage V, the output current I in equation (5) can be calculated.

It is worth noting that since the El Tayyan empirical model has only two coefficients, C_1 and C_2, it means it is a two-parameter model. This fact can be established by comparing equations (1) and (5) which yields the two parameters I_o and a of the five model parameters of a single-diode solar cell given by

$$I_o = C_1 e^{-\frac{V_{oc}}{C_2}} \tag{8}$$

$$C_2 = nV_T = a \tag{9}$$

The validity of equations (8) and (9) can be justified. Thus, equation (8) is valid since I_o has same units of current with C_1 as the exponent is dimensionless whereas equation (9) is valid since it is equal to equation (4). The modified ideality factor a of the diode is not usually available on the manufacturer's datasheet and is not easily deduced on the I-V curve which makes some authors [39, 40] to guess its value and others [41-44, 45] reduce their models to less than five parameters. The advantage of the El Tayyan model over other existing models is that it doesn't require the knowledge of the internal PV system parameters and involve less computational efforts or extra measurements. It is against this background, El Tayyan model combined with two models [39, 40] that assumed constant a produced two additional models, El Tayyan-Cubas model and El Tayyan-Senturk model. Therefore, in this work, five models are used to calculate the five model parameters (a, I_{ph}, I_o, R_s, R_{sh}) to generate model I-V curves for fifteen DSSCs for comparison purposes.

2.2 Cubas model

The Cubas model [39] assumed the ideal diode factor n=1.1 for the silicon cells studied and the modified diode factor a is given by equation (4). The following auxiliary parameters A, B, C, and D in equations (10-13) are used to calculate R_s in equation (14)

$$A = \frac{a}{I_{mp}} \tag{10}$$

$$B = \frac{V_{mp}(I_{sc}-2I_{mp})}{\left(V_{mp}I_{sc}+V_{oc}(I_{mp}-I_{sc})\right)} \tag{11}$$

$$C = \frac{V_{oc}-2V_{mp}}{a} + \frac{V_{mp}I_{sc}-V_{oc}I_{mp}}{\left(V_{mp}I_{sc}+V_{oc}(I_{mp}-I_{sc})\right)} \tag{12}$$

$$D = \frac{V_{mp}-V_{oc}}{a} \tag{13}$$

$$R_s = A[W_{-1}(Be^C) - (D + C)] \tag{14}$$

where W_{-1} is the lower branch of the Lambert W function. The remaining parameters R_{sh}, I_o. and I_{ph} are calculated by equations (15), (16), and (17) respectively.

$$R_{sh} = \frac{(V_{mp}-I_{mp}R_s)(V_{mp}-R_s(I_{sc}-I_{mp})-a)}{(V_{mp}-I_{mp}R_s)(I_{sc}-I_{mp})-aI_{mp}} \tag{15}$$

$$I_o = \left[I_{sc}\left(1+\frac{R_s}{R_{sh}}\right) - \frac{V_{oc}}{R_{sh}}\right]e^{-\frac{V_{oc}}{a}} \tag{16}$$

$$I_{ph} = I_{sc}\left(1+\frac{R_s}{R_{sh}}\right) \tag{17}$$

2.3 El Tayyan-Cubas model

In this model, the modified ideal diode factor a in Cubas model is replaced by the second characteristic coefficient El Tayyan's model i.e., $C_2=a$ and equations (10-17) remain the same.

2.4 Senturk model

This model is applicable to standard test conditions (STC) [37] and other conditions as well. This model assumes the diode factor n=1.2 and the modified ideal factor a is calculated using equation (4). Then, the experimental resistances R_{sho} and R_{so} are approximated by equations (18) and (19) respectively

$$R_{sho} = \frac{V_{mp}}{I_{sc}-I_{mp}} \tag{18}$$

$$R_{so} = \frac{V_{oc}-V_{mp}}{2I_{mp}} \tag{19}$$

Thereafter, I_{ph} and I_o are calculated by equations (20) and (21) respectively

$$I_{ph} = \frac{(R_{so}+R_{sho})I_{sc}}{R_{sho}} \tag{20}$$

$$I_o = \frac{I_{ph}-\frac{V_{oc}}{R_{sho}}}{e^{\frac{V_{oc}}{a}}-1} \tag{21}$$

and finally, R_s via Phang's model [32] and R_{sh} by equations (22) and (23) respectively.

$$R_S = R_{SO} - \frac{a}{I_o} e^{\frac{-V_{oc}}{a}} \tag{22}$$

$$R_{sh} = \frac{V_{mp} + I_{mp}R_S}{I_{ph} - I_{mp} - I_o\left(e^{\frac{V_{mp} + I_{mp}R_S}{a}} - 1\right)} \tag{23}$$

2.5 El Tayyan-Senturk model

Similarly, in this model, a in Senturk model is set equal to C_2 i.e., $a=C_2$ and equations (18-23) remain the same.

In practice, it is sometimes possible to differentiate the explicit model that produces the worst approximation to the data, but it is not possible to choose the best option with a proper criterion beyond a visual impression. For this reason, the results are usually analyzed using the normalized root mean-squared error (RMSE) denoted by in equation (24)

$$\varepsilon = \frac{1}{I_{sc}} \sqrt{\frac{1}{N} \sum_{j=1}^{N} \left(I_{cal,j} - I_j\right)^2} \tag{24}$$

Besides, the difference between the output current calculated with models and the one from the experimental data, related to the short-circuit current is given by equation (25)

$$\xi = \frac{I - I_{exp}}{I_{sc}} \tag{25}$$

3. Materials and Methods

3.1 Materials

The materials used in the work were chemicals, reagents and equipment viz: Ethanol, Titanium dioxide nano powder, Hydrochloric acid, Acetic acid, Mortar and pestle, Stainless steel mesh, Filter paper, Doctor tape C, Scanning Electron microscope, Solar energy simulator, Spectrophotometer, Magnetic stirrer, Glass bottle, Aluminium Foil, Glue, Adhesive tape, Acetone, Anhydrous alcohol, Strips of glass insulation spacers, Iodide electrolyte solution, N719 dye, plant dyes, Centrifuge machine, Sonicator, Fourier transform infrared spectrometer, Fluorine doped Tin oxide (FTO), Deionized water.

3.2 Methods

3.2.1 Extraction of plants dyes

Fourteen plants parts were selected and allowed to dry on shade for two weeks. The dried fruits and flowers were grinded into fine powder using a blinder (Walmat BLSTVB-RVO-000). 0.5 g, 1 g, and 2 g each of the selected samples were weighed on weighing balance and 5 % of the extracts were obtained respectively. The weighed powdered samples were collected in sterile 50 ml falcon tubes. 20 ml of ethanol was then added and were vortexed. The solutions were sonicated using a sonicator (Branson SFX250) for 1 h at 4^0 C. The samples were then centrifuged at 1500 rpm in 4^0 C for 10 min. The solid residues were filtered out while the supernatants of the clear dry solutions were collected, and stored at 4^0 C before use. The containers were covered with aluminium foil to prevent damage from light exposure [47,48].

3.2.2 Assemblage of solar cells

Fluorine doped tin oxide (FTO) of resistance 14 Ω/cm^2 (TCO 2215 salonix) substrate was cleaned in surfactant, deionized water, acetone and ethanol. Paste of TiO_2 was prepared with 0.25 g of TiO_2, 0.5 ml of acetic acid and mixture of deionized water and ethanol at ratio of 1:1 (10 ml), and stirred for 20 min, to prevent the agglomeration of the particles. Triton–X 0.5 ml (salonix) was added, the resultant mixture was grounded to facilitate coating of the colloid on the substrate in order to obtain homogenous paste. Doctor blade technique was adapted to coat the TiO_2 paste on FTO glass substrate with active area of 0.16 cm^2. TiO_2 coated films were sintered at 450 ^0C for 30 min. The films were cooled at room temperature. To attain sensitization of dye, films were dipped in dye like ethanolic solution of the plant dyes for 24 h. The sensitized electrodes were rinsed with ethanol to remove the unanchored dyes. Counter electrode was obtained by placing a thin layer of platisol which was squeezed printed using a polyester mesh sintered at 450 ^0C for 30 min. A drop of Iodolyte TG – 50 was casted on the surface of sensitized photo anodes, to penetrate into the porous structure via capillary action. The Pt-coated FTO electrode was then clipped onto the top of dye absorbed TiO_2 working electrode to form the complete solar cell. The photo electrochemical cell (PEC) was then mounted in a sample holder inside a metal box with an area of 1 cm^2 opening to allow light from the source. The photoelectrode and the counter electrode were overlappingly placed in a holder so that the titanium dioxide covered area of the photoelectrode was the only part of the photoelectrode that was in contact with the counter electrode. The non-titanium dioxide covered area of the photoelectrode and the non- overlapping edge of the counter electrode were connected to the measuring equipment by means of cords and crocodile clips. All experiments were carried out at ambient temperature. The image of one of the assembled cells is shown in Fig. 2.
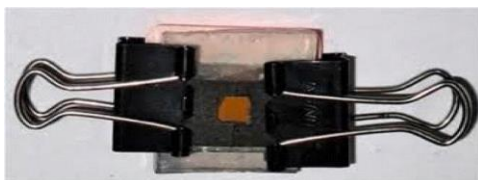

Figure 2.   Assembled DSSC

3.2.3 Characterization of extracted dyes and solar cells

The photovoltaic parameters of the fabricated DSSCs were measured using a computer controlled digital source meter (Keithley, 2400) and a solar simulator (AM 1.5 G, 100 mW cm^{-2} Oriel) as light source. The light intensity was adjusted with a reference silicon cell (PV measurement Co). The sample was masked with black opaque tape along the board of the active area. The photovoltaic parameters, open circuit voltage (V_{oc}), short circuit current *density* (I_{sc}), fill factor (FF) and overall efficiency (η) were obtained from I- V curve.

4. Results and discussion

Table 1. Characteristic parameters (I_{sc}, I_{mp}, V_{mp}, V_{oc}, P_{max}, FF, η) of the solar cells studied

Source of natural dye		Photovoltaic parameters						
English Name	**Scientific Name**	I_{sc} (mA)	I_{mp} (mA)	V_{mp} (V)	V_{oc} (V)	P_{max} (mW)	FF	η %
Control	TiO$_2$/N719	9.355	7.574	0.4	0.590	3.028	0.54	3.02
Witch seed flower	Striga hermonthica	1.970	1.379	0.4	0.639	0.551	0.43	0.55
Bitter gourd	Momordica charantia	9.244	6.450	0.4	0.536	2.580	0.51	2.57
Bougainvillea	Bougainvillea	3.450	2.783	0.3	0.484	0.834	0.50	0.83
Flamboyant	Delonix regia	1.717	1.442	0.4	0.610	0.576	0.55	0.57
Wild marigold	Calendula arvensis	1.600	0.957	0.3	0.504	0.287	0.35	0.28
Red cockscomb	Celosia cristata	1.580	1.290	0.3	0.490	0.387	0.49	0.38
Lantana	Lantana camera	1.530	1.262	0.4	0.600	0.504	0.54	0.50
Hibiscus	Hibiscus rosa sinensis	1.480	1.090	0.3	0.450	0.327	0.49	0.32
Sun flower	Helianthus	1.590	1.081	0.4	0.530	0.432	0.51	0.43
Rose flower	Rosa	1.690	1.283	0.4	0.563	0.512	0.53	0.51
Orange peel	Citrus aurantium	1.400	1.121	0.2	0.370	0.224	0.43	0.22
Tomato	Lycopersicon esculentum	0.230	0.135	0.2	0.290	0.027	0.40	0.03
Mango peel	Mongifera indica	2.51	2.130	0.4	0.618	0.852	0.76	1.00
Guava peel	Psidium guajava	0.900	0.669	0.3	0.452	0.201	0.49	0.20

Table 1 depicts the characteristic parameters of the solar cells studied. The results show that the DSSC with witch seed flower dye has the highest conversion efficiency 2.57 %, second mango peel 1 %, and third bougainvillea 0.83 % after the standard cell 3.02 %. In this paper, I-V curve matching is done only for measured and calculated model data from these four solar cells for clarity. Using the values of the characteristic points (I_{sc}, I_{mp}, V_{oc}, V_{mp}) in Table 1, the El Tayyan coefficients or model parameters were computed (Table 2).

Table 2. El Tayyan model parameters of the solar cells studied

Source of natural dye		El Tayyan model parameters				
English Name	Scientific Name	C_1	C_2	$a=C_2$	n	I_o (A)
Control	TiO$_2$/N719	0.009838	0.195796	0.195796	7.5626	4.833×10^{-4}
Witch seed flower	Striga hermonthica	0.009700	0.062867	0.062867	2.4282	1.872×10^{-4}
Bitter gourd	Momordica charantia	0.009245	0.060393	0.060393	2.3327	1.293×10^{-6}
Bougainvillea	Bougainvillea	0.003927	0.229684	0.229684	8.8715	4.775×10^{-4}
Flamboyant	Delonix regia	0.001862	0.238962	0.238962	9.2299	1.450×10^{-4}
Wild marigold	Calendula arvensis	0.001777	0.218650	0.218650	8.4453	1.773×10^{-4}
Red cockscomb	Celosia cristata	0.001830	0.246337	0.246337	9.5148	2.504×10^{-4}
Lantana	Lantana camera	0.001632	0.216544	0.216544	8.3640	1.022×10^{-4}
Hibiscus	Hibiscus rosa sinensis	0.001558	0.150090	0.150090	5.7972	7.769×10^{-5}
Sun flower	Helianthus	0.001590	0.054753	0.054753	2.1148	9.943×10^{-8}
Rose flower	Rosa	0.001695	0.095372	0.095372	3.6837	4.628×10^{-6}
Orange peel	Citrus aurantium	0.001946	0.291046	0.291046	11.2416	5.457×10^{-4}
Tomato	Lycopersicon esculentum	0.000230	0.043932	0.043932	1.6969	3.130×10^{-7}
Mango peel	Mongifera indica	0.002760	0.257501	0.257501	9.9459	2.504×10^{-4}
Guava peel	Psidium guajava	0.000951	0.154409	0.154409	5.9640	5.091×10^{-5}

Using the values of the characteristic points in equations (6) and (7), the numerical values of the El Tayyan coefficients or model parameters (C_1, C_2) were computed (Table 2). The emergence of the two coefficients suggests that the El Tayyan model is a two-parameter model, the parameters being the modified ideal diode factor a and the diode saturation current I_o which are related to C_1 and C_2 via equations (8) and (9). Equation (8) shows I_o is function of both C_1 and C_2 whereas equation (9) reveals a is equal to C_2. The values of I_o and a were computed using equations (8) and (9) respectively. The results show all the parameters are regular i.e. they have positive values. Furthermore, a depends on the type of dye used to fabricate the solar cell. Thus, in our model, the El Tayyan modified ideal factor $C_2=a$, is used to generate a set of four model parameters (I_o, I_{ph}, R_s, R_{sh}) for systems where previous researchers assumed the diode ideal factor constant, n=1.1 [39] and n=1.2 [40] for comparison purpose (Table 3).

Table 3. El Tayyan-Cubas model parameters for the solar cells studied

Natural dye	Cubas/El Tayyan model parameters, n or a not constant					Cubas model parameters n=1.1 or a=0.028479			
English Name	a	R_s (Ω)	R_{sh} (Ω)	I_o (A)	I_{ph} (mA)	R_s (Ω)	R_{sh} (Ω)	I_o (A)	I_{ph} (mA)
Control	0.1958	-0.8	-109.9	7.27×10^{-4}	9.42	15.8	339.5	8.10×10^{-12}	9.79
Witch seed flower	0.0629	42.0	-245.8	3.67×10^{-4}	1.63	124.3	711.0	2.55×10^{-13}	2.31
Bitter gourd	0.0604	-0.4	184.8	8.84×10^{-7}	9.22	8.3	152.7	4.18×10^{-11}	9.75
Bougainvillea	0.2297	30.0	-22.0	2.52×10^{-3}	-1.25	45.8	1160.0	1.32×10^{-10}	3.59
Flamboyant	0.2390	19.1	-239.7	3.21×10^{-4}	1.58	99.4	2993.6	7.83×10^{-13}	1.77
Wild marigold	0.2187	94.8	57.1	7.75×10^{-4}	-1.06	146.8	375.2	1.82×10^{-11}	2.23
Red cockscomb	0.2463	87.7	-20.0	2.62×10^{-3}	-5.34	104.5	3568.7	5.02×10^{-11}	1.63
Lantana	0.2165	7.3	-420.7	1.83×10^{-4}	1.50	104.3	2562.1	9.62×10^{-13}	1.59
Hibiscus	0.1501	-5.6	-1052.3	9.55×10^{-5}	1.49	77.7	981.3	1.56×10^{-10}	1.60
Sun flower	0.0548	-3.5	957.6	6.44×10^{-8}	1.58	42.0	829.4	8.53×10^{-12}	1.67
Rose flower	0.0954	0.7	3032.4	4.11×10^{-6}	1.69	68.0	1185.0	3.41×10^{-12}	1.79
Orange peel	0.2910	131.6	21.5	-2.03×10^{-3}	9.97	123.0	-584.4	3.96×10^{-9}	1.11
Tomato	0.0839	-92.1	2457.0	1.40×10^{-7}	2.21	107.5	2171.9	4.08×10^{-9}	0.24
Mango peel	0.2575	20.7	-115.0	6.71×10^{-4}	2.06	71.6	2552.7	8.80×10^{-13}	2.58
Guava peel	0.1544	-3.0	-1317.4	6.67×10^{-5}	9.02	130.7	1707.1	9.01×10^{-11}	0.97

Table 3 contains two model parameters generated from Cubas model for n fixed or constant (n=1.1) for all solar cells and Cubas-El Tayyan model for n varying with dyes or photosensitizers used in fabricating the solar cells. For the Cubas-El Tayyan model, all the model parameters except a manifest parameters' irregularities i.e. the parameters have both negative and positive values. The number of negatives values are 0, 6, 9, 1, 3 for the parameters a, R_S, R_{sh}, I_o, I_{ph} respectively. Also, the two models produce different values for all the model parameters except I_{ph} have same values and I_o values for Cubas model have smaller values compared to those of Cubas-El Tayyan values. Furthermore, the values of I_{ph} in Table 3 are not equal to the values of I_{sc} in Table 1 but they are of the same order of magnitude.

Table 4. El Tayyan-Senturk model parameters for the solar cells studied.

| Natural dye	Senturk/El Tayyan model parameters, n or a not constant	Senturk model parameters n=1.2, a=0.031068

| English Name	a	R_s (Ω)	R_{sh} (Ω)	I_o (A)	I_{ph} (mA)	R_s (Ω)	R_{sh} (Ω)	I_o (A)	I_{ph} (mA)
Control	0.1958	-13.1	319.8	3.74×10^{-4}	9.877	8.3	211.8	4.10×10^{-11}	9.877
Witch seed flower	0.0629	82.1	21.5	5.38×10^{-7}	2.222	84.4	20.2	1.62×10^{-11}	27.186
Bitter gourd	0.0604	0.8	145.1	8.63×10^{-7}	9.930	5.5	134.0	1.98×10^{-10}	9.930
Bougainvillea	0.2297	-43.7	361.0	3.64×10^{-4}	3.704	21.2	411.1	4.51×10^{-10}	3.704
Flamboyant	0.2390	-86.5	2550.0	1.17×10^{-4}	1.803	50.4	1372.6	4.11×10^{-12}	1.803
Wild marigold	0.2187	-115.8	216.6	9.82×10^{-5}	1.966	71.5	369.4	7.98×10^{-11}	1.966
Red cockscomb	0.2463	-100.8	807.3	1.93×10^{-4}	1.692	48.2	946.5	1.72×10^{-10}	1.692
Lantana	0.2165	-88.6	2316.8	8.07×10^{-5}	1.611	53.5	1407.5	4.96×10^{-12}	1.611
Hibiscus	0.1501	-70.0	664.0	5.39×10^{-5}	1.612	38.6	697.2	5.26×10^{-10}	1.612
Sun flower	0.0548	7.3	785.9	6.54×10^{-8}	1.712	30.2	738.9	4.05×10^{-11}	1.712
Rose flower	0.0954	-14.1	1139.4	3.36×10^{-6}	1.799	38.2	925.8	1.65×10^{-11}	1.799
Orange peel	0.2910	-127.1	169.6	4.02×10^{-4}	1.548	45.7	621.1	6.94×10^{-9}	1.548
Tomato	0.0839	-7.4	1724.8	1.74×10^{-7}	0.266	91.9	1757.7	1.14×10^{-8}	0.266
Mango peel	0.2575	-63.3	1966.7	2.04×10^{-4}	2.632	36.0	992.1	4.70×10^{-12}	2.632
Guava peel	0.1544	-118.1	1126.6	3.57×10^{-5}	0.979	64.3	1179.6	3.03×10^{-10}	0.979

Table 4 depicts the values of model parameters generated from two models, Senturk model for n fixed (n=1.2) and Senturk-El Tayyan model for n varying for all solar cells. For the Senturk-El Tayyan model, all the model parameters are regular except R_S has 13 values negative i.e. only R_s manifests parameter irregularity. Also, all the El Tayyan model parameters differ from that of Cubas model parameters except I_{ph} values. However, the I_{ph} values differ from I_{sc} values (Table 1) and the I_o values for both models (Table 4) differ from those of El Tayyan in Table 2. Thus, the overall results show that the number of parameter irregularity vary with model. The acceptance of the significance of the parameter irregularity lies in the validity of the fitness between the model data and measured data I-V curves. However, in this paper, the fitting of I-V curves is done for only the first four solar cells with high efficiencies for clarity.
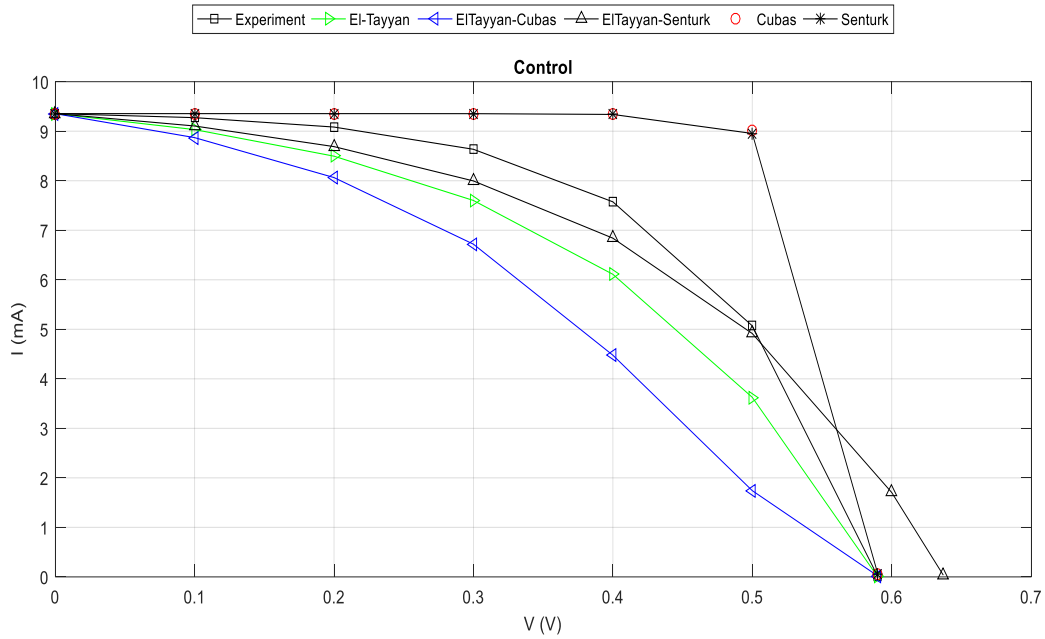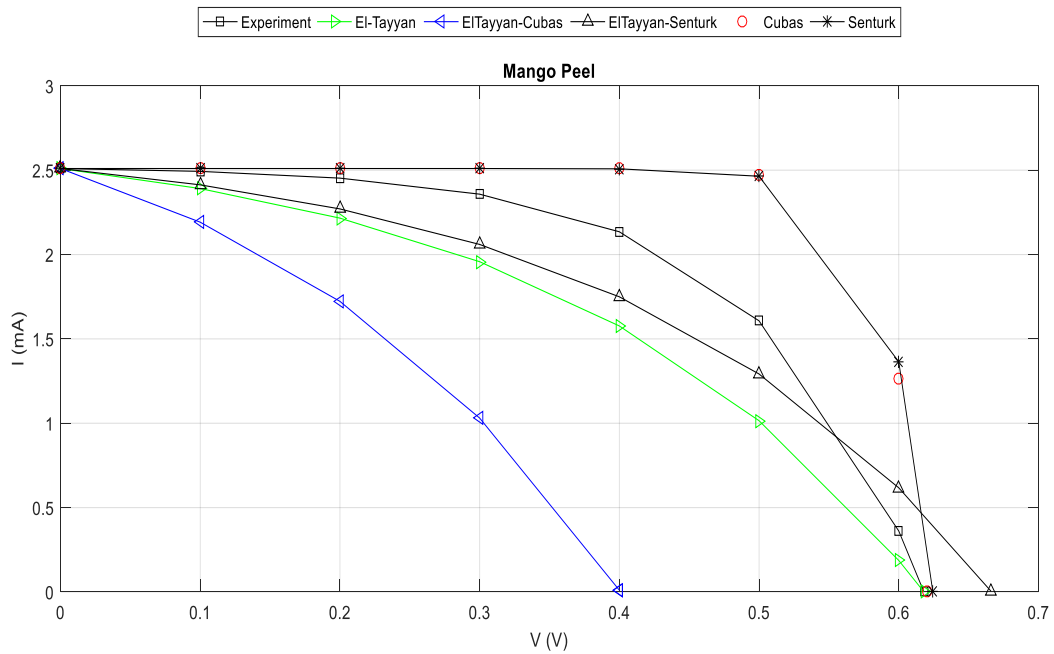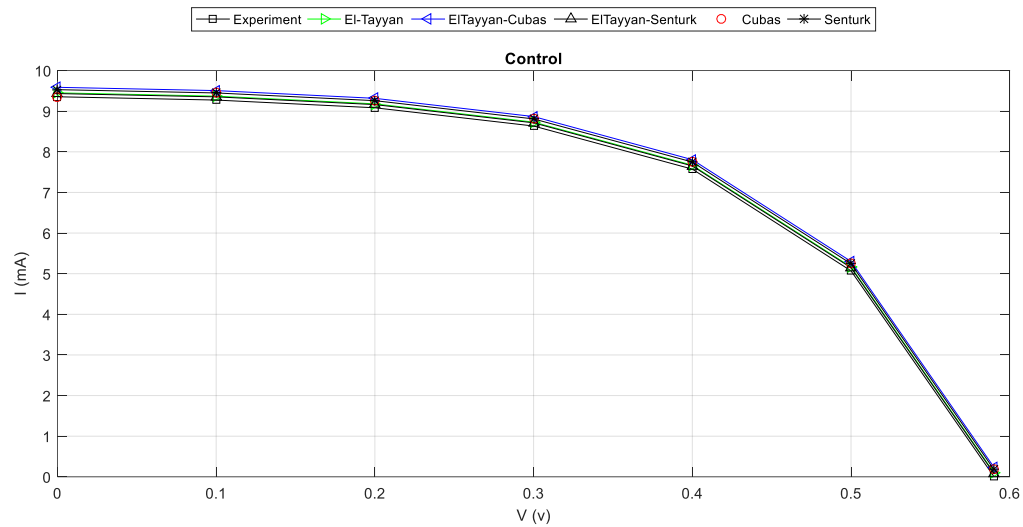
(a) Standard
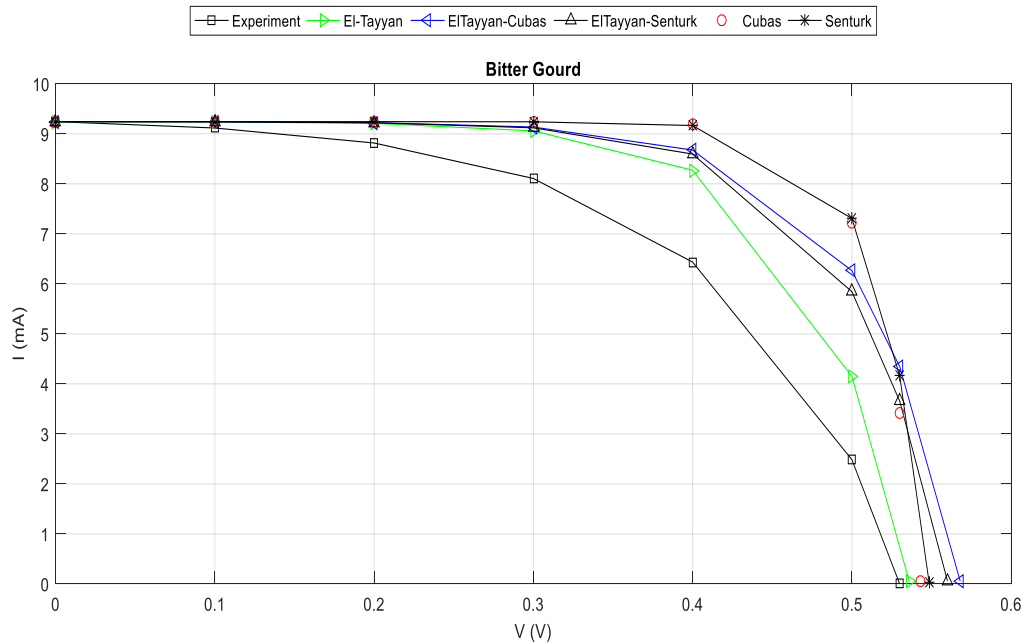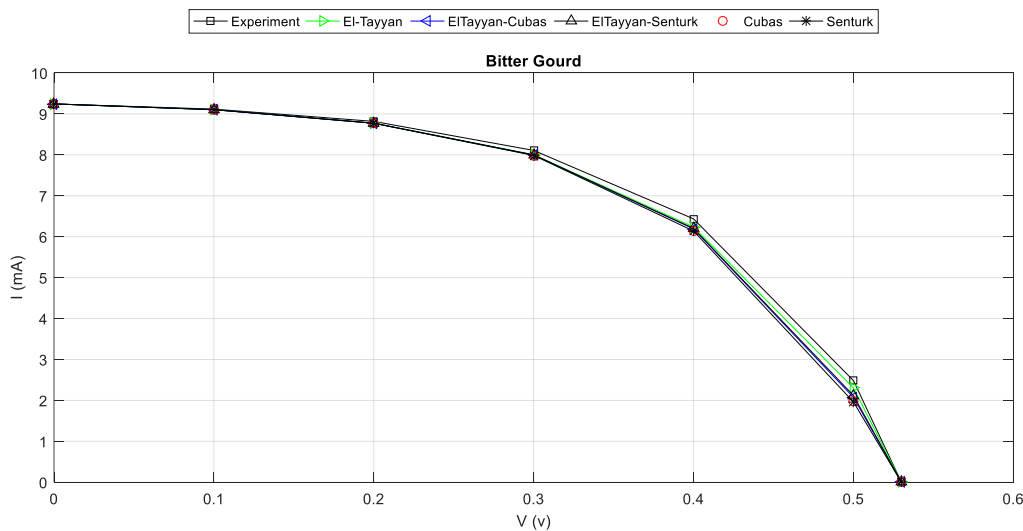

(b) Bitter gourd
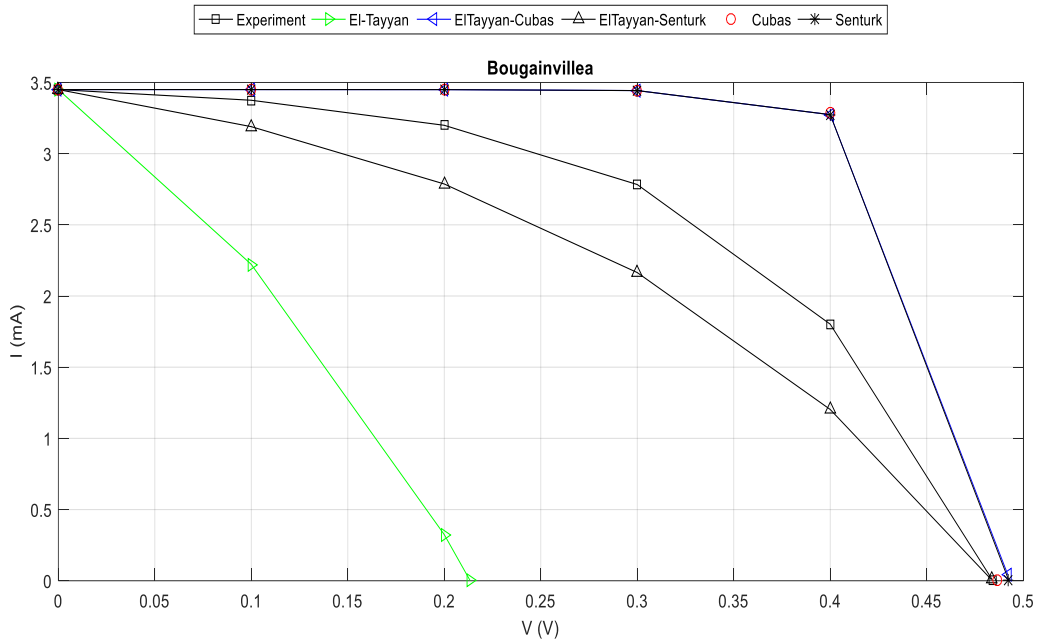
(c) Bougainvillea

(d) Mango Peel

Figure 3. Curves for the explicit models analyzed, fitted to the (a) standard (control) (b) bitter gourd (c) bougainvillea and (d) mango solar cells data using the analytical methods proposed.

Figures 3(a-d) depict the I-V curves of solar cells (a) control (b) bitter gourd (c) bougainvillea and (d) mango for measured data and five models: El Tayyan, El Tayyan-Cubas, El Tayyan-Senturk, Cubas, and Senturk. The figures show the I-V curves are at constant current source at low voltages with a current approximately equal to the short-circuit current, I_{sc}. With increasing voltage at a certain point, the current begins to drop off exponentially to zero at open-circuit voltage, V_{oc}. The values of V_{oc} varies with DSSC as well as model which is distinctly shown in (a) El Tayyan model and in (a/d) El Tayyan-Cubas model. Over the entire voltage range, there is one point where the cell operates at the highest efficiency; this is the maximum power point, MPP (V_{mp}, I_{mp}). The system design is to operate the cell at that point. However, the system design is complicated by the fact that the maximum power point varies with irradiance and temperature. It is worth noting the MPP changes with model.
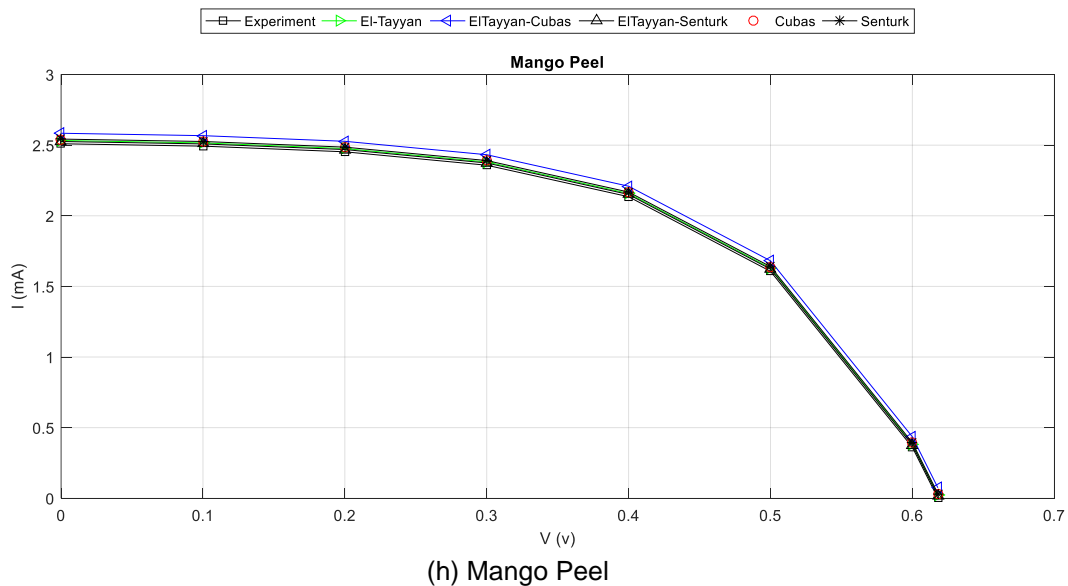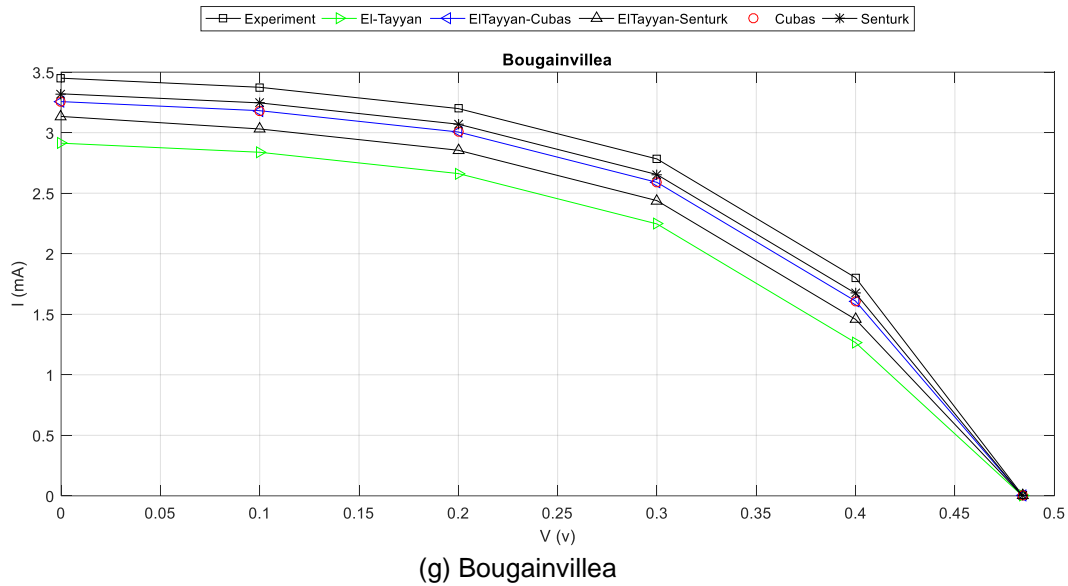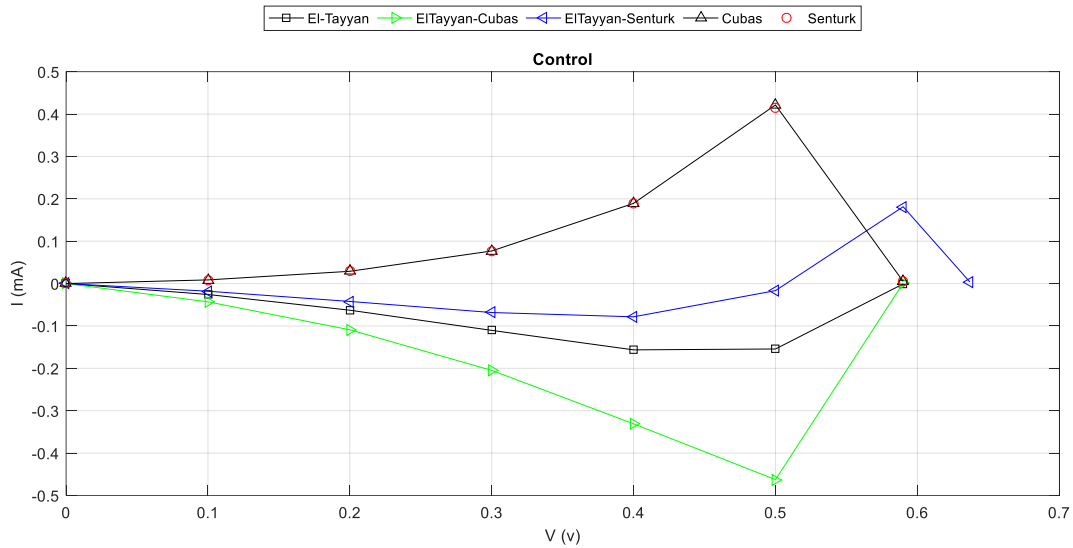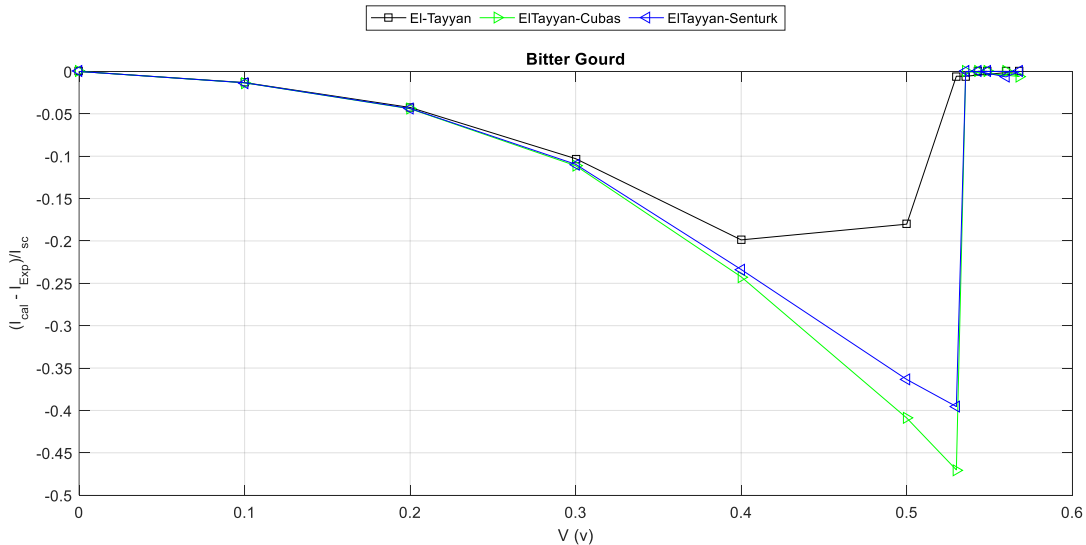

(e) control

(f) Bitter gourd

(g) Bougainvillea

(h) Mango Peel

Figure 4.   Curves for the explicit models analyzed taking error into account, fitted to the (e) standard (control) (f) bitter gourd (g) bougainvillea and (h) mango solar cells data using the analytical methods proposed.

Figs. 4(e-h) depict best I-V curve fits after eliminating the error between output current model and measured current. The values ε of the normalized root mean squared error (NRMSE) of the output currents were generated using equation (24) which lie in the range $0.015 << \varepsilon << 0.536$ for all DSSCs and models. Based on the fact that the best model has the smallest value of ε, our results
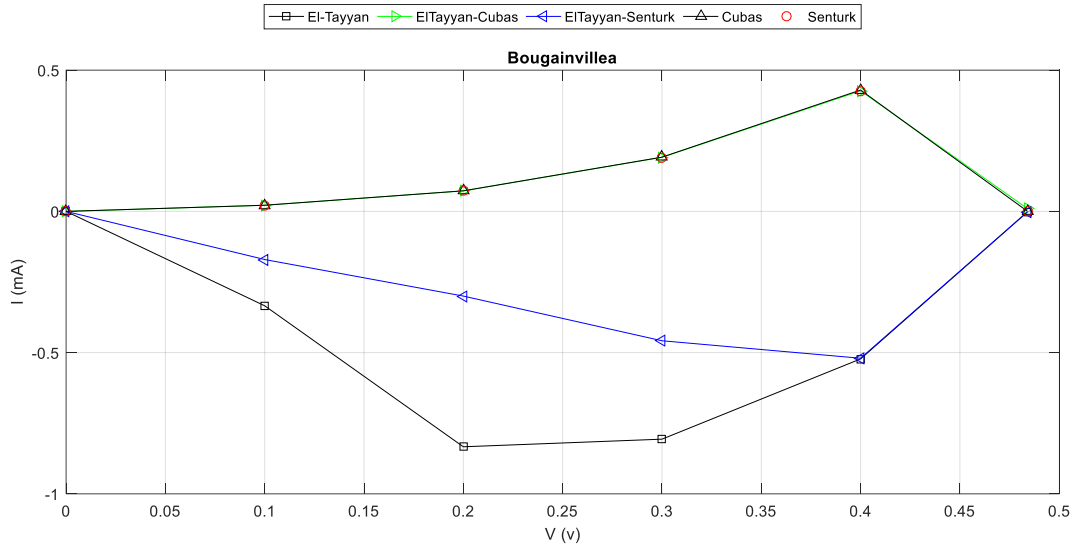
show that DSSC/best model as follows: DSSC control/El Tayyan model ε=0.078, DSSC bitter gourd/El Tayyan model ε=0.109, DSSC bougainvillea/Senturk model ε=0.129, and DSSC mango/El Tayyan-Senturk model ε=0.015.
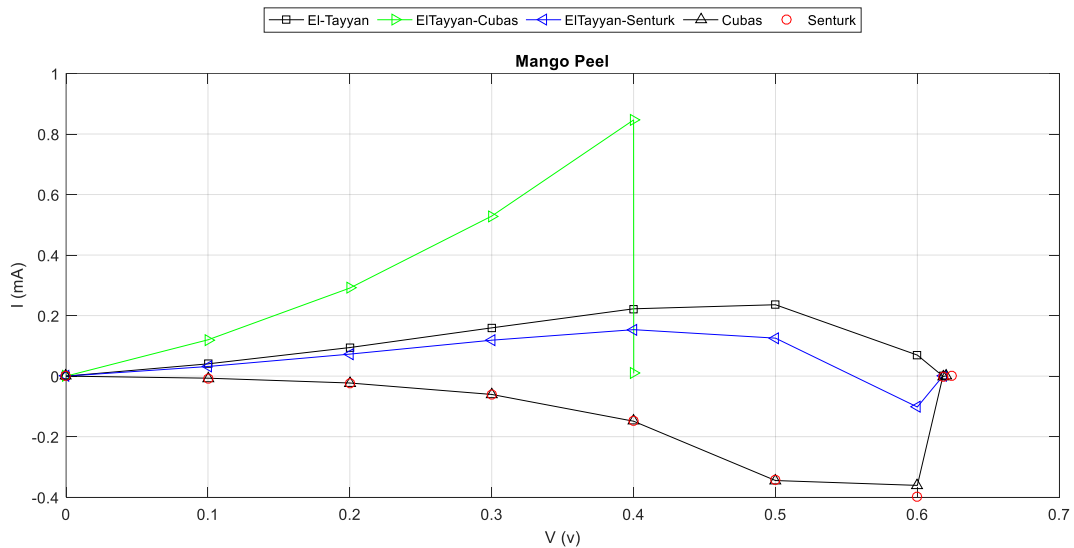

(i) Control

(j) Bitter Gourd

(k) Bougainvillea

(l) Mango Peel

Figure 5. Fig. 5 Curves for output current errors in relation to short circuit current for the explicit models (i) control (j) bitter gourd (k) bougainvillea and (l) mango solar cells data.

The differences between the output currents calculated with models using equation (25) mand output currents measured in relation to the short-circuit current and Figs. 5(i-k) depict current differences for the models and DSSCs studied.

Conclusion

In this paper, the El Tayyan empirical formula in conjunction with other exponential PV model equations were used to obtain the value of the modified ideal diode factor instead of assuming its value a constant as proposed by some authors [39, 40]. Five models, El tayyan, El Tayyan-Cubas, El Tayyan-Senturk, Cubas, and Senturk were employed to extract the five model parameters for fifteen DSSCs. The results show that in terms of conversion efficiency, next to the standard solar cell, the most efficient DSSCs are the ones with photosensitizers namely bitter gourd, bougainvillea, and mango. Also, the results reveal all the model parameters are regular for El Tayyan model while they are irregular with varying degrees for the rest of the models. In addition, despite the parameter irregularities, there is good match between the model data and measured data I-V curves meaning presence of irregular parameters may not be undesirable for some applications. Thus, the irregularities associated with the extracted parameters revealed by these methods can serve as a useful assessment criterion and tool for researchers and engineers in deciding the proper extraction method for their application.

References

[1]   Pfann, W.; Van Roosbroeck, W. Detailed balance limit of efficiency of p-n junction solar cells. J. Appl. Phys. 25 (1954) 1422

[2]   Prince, M. B. Silicon solar energy converters. J. Appl. Phys. 26 (1955) 534-540.

[3]   Iles, P.A.; Leibenhant, B. Solid-state electron. IRE Trans. Mil. Electron, MIL.-6 (1962) 5.

[4]   Wolf, M.; Rauschenbach, H. Series resistance effects on solar cell measurements. Adv. Energy convers. 3 (1963) 455.

[5]   Sze, S. M. Physics of semiconductor devices, John Wiley and Sons, New York, 1969.

[6]   Rauschenbach, H. Solar cell array design handbook vol I, Jet propulsion laboratory, California Institute of Technology. Pasadena, California 91103, 1976

[7]   Van Dyk, E. E.; Meyer, E. I. Analysis of the effect of parasitic resistances on the performance of on photovoltaic modules. Renewable Energy 29 (2004) 333

[8]   de Blas, M. A.; Torres, J. I.; Prieto, F.; Garcia, A. Selecting a suitable model for characterizing photovoltaic devices. Renewable Energy 25 (2002) 371.

[9]   Carrero, C.; Rodriguez, J.; Platero, C. Simple estimation of PV modules loss resistances for low error modeling. Renewable Energy 35 (2010) 1103-1108.

[10] Zhu, X-C.; Flu, Z-H.; Long, X-M. Sensitivity analysis and more accurate solution of photovoltaic solar cell parameters. Sol. Energy 85 (2011) 393.

[11] Batzner, D. I.; Bomeo, A.; Zogg, H.; Tiwari, A. N. in 17-th EC PV Solar Energy Conference, Munich, Germany, 2001, pp1-4.

[12] Kennerad, K. I. Analysis of performance degradation in CDS solar cells. IEEE Trans. Aerops. Electron Syst. 5 (1969) 912.

[13] Charles, J.; Abidelkrim, M.; Muoy, Y.; Mialhe, P. Method of analysis of the current-voltage characteristics of solar cells. Sol. Cells 4 (1981) 169.

[14] Easwarakhanthan, T.; Botrin, J.; Bouhouch, I.; Boutrit, C. Nonlinear minimization algorithm for determining the solar cell parameters with microcomputers. Int. J. Sol. Energy 4 (1986) 1.

[15]   Eikelboom, J. A.; Reinders, A. H. M. E. Determination of the irradiation dependent efficiency of multicrystalline Si PV modules on basis of IV curve fitting and its influence on the annual performance, in proceedings of the 4th European PV Solar Energy Conference, 1997, pp293-296.

[16]   Villalva, M. G.; Gazoli, J. R.; Filho, F.R. Comprehensive approach to modeling and simulation of photovoltaic arrays. IEEE Trans. Power Electron 24 (2009) 1198-1208.

[17]   Villalva, M. G.; Gazoli, J. R.; Filho, F. R. Modeling and circuit-based simulation of photovoltaic arrays. Brazilian Power Electronics Conference 2009, p. 1244.

[18]   LI, Y.; Huang, W.; Huang, H.; Hewitt, C.; Chen, Y.; Fang, G.; Carroll, D. I. Evaluation of methods to extract parameters from current-voltage characteristics of solar cells. Sol. Energy 90 (2013) 51.

[19]   Das, A. K. An explicit J-V model of a solar cell for simple fill factor calculation. Sol. Energy 85 (2011) 1906.

[20]   Peng, I.; Sun, Y.; Meng, Z.; Wang, Y.; Xu, Y. A new method for determining the characteristics of solar cells. J. Power sources 227 (2013) 131.

[21]   AlRashidi, M. R.; AlHajri, M. F.; El-Naggar, K. M.; Al-Othman, A. K. A new estimation approach for determining I-V characteristics of solar cells. Sol. Energy 85 (2011) 1543.

[22]   Askarzadeh, A.; Rezazadeh, A. Parameter extraction of solar photovoltaic modules using penalty-based differential evolution. Sol. Energy 86 (2012) 3241

[23]   Askarzadeh, A.; Rezazadeh, A. Artificial bee swarm optimization for parameters identification of solar cell models. Appl. Energy 102 (2013) 943

[24]   AlQahtani, A. A simplified and comprehensive approach to characterize photovoltaic system performance. Energytech. IEEE., Cleverland, Ohio, 2012, pp. 1-6, nd.

[25]   Averbukh, M.; Lineykin, S.; Kuperman, A. Five-parameter model of photovoltaic cell based on STC data and dimensionless. Prog. Photovoltaics Res. Appl. 21. (2012) 1016.

[26]   Chatterjee, A.; Keyhani, A.; Kapoor, D. Identification of photovoltaic source models. IEEE Trans. Energy convers. 26 (2011) 883.

[27]   Das, A. K. Analytical expression of the physical parameters of an illuminated solar cell using explicit J-V model. Renewable Energy 52 (2013) 95.

[28]   Lineykin, S.; Averbukh, M.; Kuperman, A. An improved approach to extract the single-diode equivalent circuit parameters of a photovoltaic cell/panel. Renew. And SUS. Energy Reviews. 30, 282-289, 2014.

[29]   Kuo, Y.; Liang, J. T.; Chen, J. Novel maximum power point tracking controller for photovoltaic energy conversion system. IEEE Trans. Ind. Electron. 48 (2001) 594.

[30]   Walker, G. Evaluating MPPT converter topologies using MATLAB PV model. J. Electr. Electron. Eng. 21 (2001). 49.

[31]   Chan, D. S. H.; Phang, J. C. H. Analytical methods for the extraction of solar cell single and double diode model parameters from I-V characteristics. IEEE Trans. Electron Dev. 34 (1987) 286.

[32]   Phang, J. C. H.; Chan, D. S. H.; Phillips, J. R. Accurate analytical method for the extraction of solar cell model parameters. Electron lett. 20 (1984) 406.

[33] Lo Brano, V.; Orioli, A.; Ciulla, G.; Gangi, A. D. An improved five-parameter model for photovoltaic modules. Sol. Energy Mater. Sol. Cells 94 (2010) 1358.

[34] Di Piazza, M.; Vitale, G. Photovoltaic sources: Modeling and emulation, Springer, London, 2013.

[35] El Tayyan, A.; Al-Aqsa, J. An empirical model for generating the IV characteristics for a photovoltaic system. Uni. 10 (S. E.) 2006.

[36] Saleem, H.; Karmalkar, S. An analytical method to extract the physical parameters of a solar cell from four points on an illuminated J-V curve. IEEE Electron device lett. 2009, 30 349-352.

[37] Saloux, E.; Teyssedou, A.; Sorin, M. Explicit model of photovoltaic panels to determine voltages and current at the maximum power point. Sol. Energy 2011, 85, 713-722.

[38] Khan,F.; Back, S. H.; Kim, J. H. Extraction of diode parameters of silicon solar cells under high illumination conditions. Energy convers. Manag. 2013, 76, 421-429.

[39] Cubas, J.; Pindado, S.; Victoria, M. On the analytical approach for modeling photovoltaic systems behavior.J. power sources 2014, 247, 467-474.

[40] Senturk, A.; Eke, R. A new method to simulate photovoltaic performance of crystalline silicon photovoltaic modules based on datasheet values. Renew. Energy 2017, 103, 58-69.

[41] Sera, D.; Teodorescu, R.; Rodriguez, P. in: IEEE INT. Symposium on Industrial Electronics (ISIE), 2007, pp. 2392-2395.

[42] Khezzar, R.; Zereg, M.; Khezzar, A. Modeling improvement of the four-parameter model for photovoltaic modules. Solar Energy 110, 2014, 452-462.

[43] Aldawane, B. Modeling, simulation and parameters estimation for photovoltaic module. In proceedings of the 2014 1st Internatinal Conference on Green Energy ICGE 2014, Sfax, Tunisia, 25-27 March 2014; pp. 101-106.

[44] Cannizzaro, S.; Di Piazza, M. C.; Luna, M.; Vitale, G. PVID: An interative matlab application for parameter identification of complete and simplified single-diode PV modules. In proceedings of the 2014 IEEE 15th workshop on Control and Modeling for Power Electronics (COMPEL), Santander, Spain, 22-25 June 2014.

[45] Orioli, A.; Di Gangi, A. A procedure to calculate the five-parameter model of crystalline silicon photovoltaic modules on the basis of the tabular performance data. Appl. Energy 102 (2013) 1160.

[46] Gow, A.; Manning, C. D. (1999) Development of a photovoltaic array model for use in power-electronics simulation studies. IEEE proceedings-electric power applications, 146, 193-200.

[47] A. Babangida, J.B. Yerima, A.D. Ahmed, S.C. Ezike, Strategy to select and grade efficient dyes for enhanced photo-absorption, Afr. Sci. Rep. 1 (2022) 16–22.

[48] J.B. Yerima, A. Babangida, S.C. Ezike, W. Dunama, A.D. Ahmed, Matrix method of determining optical energy bandgap of natural dye extracts, J. Appl. Sci. Environ. Manage., 26 (5) 943–948.